Optimal Reactive Power Dispatch with Voltage-Dependent Loads using an Enhanced Butterfly Optimization Algorithm

XIOMARA CAROLINA MORALES QUINTERO, SERGIO RAUL RIVERA RODRIGUEZ
Departamento de Ingeniería Eléctrica y Electrónica
Universidad Nacional de Colombia
Ave Cra 30 #45-3 Bogotá D.C.
COLOMBIA

Abstract: - This paper presents an Algorithm for solving the Optimal Reactive Power Dispatch problem under exponential load modeling. Traditional formulations assume constant power demands, which neglect the voltage-dependent nature of real-world loads. In this work, we incorporate an exponential load model that accurately represents residential, commercial, industrial, and rural consumption patterns. The proposed EBOA combines the standard BOA with crossover mechanisms to improve exploration and exploitation capabilities. The algorithm is tested on the IEEE 30-bus system using both the traditional constant-power model and the proposed exponential load representation. Compared to conventional constant-power modeling, the exponential model reduces active power losses by up to 24.7%, improves voltage deviation by 91.1%, and enhances voltage stability by approximately 38% in the IEEE 30-bus system. These results highlight that incorporating voltage-dependent characteristics leads to more realistic and economically efficient reactive power dispatch solutions.

Key-Words: - Optimal Reactive Power Dispatch (ORPD); Exponential Load Model; Voltage-Dependent Loads; Enhanced Butterfly Optimization Algorithm (EBOA); Metaheuristics; Power Loss Minimization; Voltage Stability; IEEE 30-Bus System.

Received: May 18, 2025. Revised: January 4, 2026. Accepted: March 23, 2025. Published: June 12, 2026.

1 Introduction

Optimal Reactive Power Dispatch (ORPD) is a central optimization problem in power system operation, aiming to minimize active power losses, enhance voltage profiles, and improve system stability through the coordinated adjustment of generator voltages, transformer tap ratios, and shunt compensation devices, [1], [2]. Conventional ORPD formulations typically rely on the constant-power load assumption, where active and reactive demand remain fixed regardless of bus voltage magnitude, [3]. Although computationally convenient, this simplification does not accurately reflect the behavior of real electrical loads.

In practical networks, residential, commercial, industrial, and agricultural loads exhibit diverse degrees of voltage dependency. Residential appliances and lighting loads are particularly sensitive to voltage variations, while industrial motor-driven loads follow nonlinear voltage–current relationships, [4]. Ignoring these characteristics may lead to incorrect estimation of system losses, unrealistic voltage profiles, and suboptimal dispatch solutions, especially under stressed or low-voltage conditions, [5].

To address these limitations, this work incorporates an exponential voltage-dependent load model into the ORPD formulation, [6]. This representation captures a wide spectrum of load categories using a compact mathematical structure, while introducing additional nonlinearities that increase the complexity of the optimization landscape. Consequently, solving ORPD under voltage-dependent loads requires advanced metaheuristics with strong exploration and exploitation capabilities, [7].

In this context, we propose an Enhanced Butterfly Optimization Algorithm (EBOA), which augments the standard BOA by integrating crossover operators inspired by the Exchange Market Algorithm together with a non-uniform mutation mechanism. These modifications strengthen population diversity during early iterations and improve convergence accuracy near the optimal region, making the algorithm more suitable for nonlinear ORPD scenarios, [8].

The main contributions of this paper can be summarized as follows:

- A detailed formulation of an exponential voltage-dependent load model that represents the behavior of residential, commercial, industrial, and rural loads.
- An ORPD framework that explicitly accounts for voltage-dependent loads and highlights their impact on optimal dispatch decisions.
- A hybrid enhancement of the Butterfly Optimization Algorithm through EMA-based crossover and non-uniform mutation, improving both exploration and convergence performance.
- A comprehensive comparative study between constant-power and exponential load models using the IEEE 30-bus test system, including analyses of losses, voltage deviation, voltage stability, and reactive power allocation.
- Integration of sensitivity analyses, convergence behavior, and voltage profile evaluation to assess the robustness and efficiency of the proposed EBOA under nonlinear load conditions.

The remainder of this paper is organized as follows. Section 2 presents the mathematical formulation of the voltage-dependent load model and the ORPD problem. Section 3 describes the proposed EBOA algorithm. Section 4 outlines the simulation setup. Section 5 discusses the numerical results and sensitivity analyses. Section 6 concludes the paper.

2 Exponential Load Modeling

The voltage dependency of loads is represented using exponential models, where active and reactive power demands vary with the bus voltage magnitude. This formulation is a compact approximation of the more general ZIP model and captures voltage-sensitive behavior more accurately than the constant power model, [9], [10].

2.1 General Exponential Model

The active and reactive power demands at bus i are expressed as (equation 1 and equation 2), [11], [12]:

$$P_{D_i} = P_{D_{0_i}} \left(\frac{V_i}{V_{0_i}} \right)^{\alpha_i} \tag{1}$$

$$Q_{D_i} = Q_{D_{0_i}} \left(\frac{V_i}{V_{0_i}} \right)^{\beta_i} \tag{2}$$

where $P_{D_{0_i}}$ and $Q_{D_{0_i}}$ are the nominal active/reactive power demands at nominal voltage V_{0_i}, V_i is the actual bus voltage, and α_i, β_i are the exponential coefficients. A compact formulation of the complex load demand is (equation 3), [13]:

$$S_{D_i}(V_i) = P_{D_i}(V_i) + jQ_{D_i}(V_i). \tag{3}$$

2.2 Load Type Parameters

Different load categories exhibit distinct voltage–power sensitivities, [14], [15]:

2.2.1 Residential Loads

$$\alpha_{\text{res}} = 1.5, \qquad \beta_{\text{res}} = 2.5$$

2.2.2 Commercial Loads

$$\alpha_{\text{com}} = 1.2, \qquad \beta_{\text{com}} = 2.0$$

2.2.3 Industrial Loads

$$\alpha_{\text{ind}} = 0.8, \qquad \beta_{\text{ind}} = 1.5$$

2.2.4 Rural/Agricultural Loads

$$\alpha_{\text{rural}} = 1.8, \qquad \beta_{\text{rural}} = 3.0$$

In the case of mixed loads at a bus, composite coefficients can be defined as weighted averages based on the proportion of each load type. Finally, we have the following definition:

Definition 1 (Exponential Load Sensitivity)**.** *The sensitivity of a load's active power consumption to changes in bus voltage is defined by its partial derivative with respect to voltage, given by (equation 4):*

$$\frac{\partial P_{D_i}}{\partial V_i} = \frac{\alpha_i}{V_{0_i}} P_{D_{0_i}} \left(\frac{V_i}{V_{0_i}} \right)^{\alpha_i - 1} \tag{4}$$

A larger exponent α_i indicates a load type with higher voltage sensitivity, such as residential or rural loads, meaning its power consumption changes more drastically with voltage fluctuations compared to less sensitive loads like industrial motors.

3 Problem Formulation

The ORPD problem with exponential loads is formulated as a constrained nonlinear optimization problem, [16].

3.1 Objective Functions

We consider three objective functions:

3.1.1 Active Power Loss Minimization

$$\min f_1 = \sum_{k=1}^{N_l} G_k \left(V_{i(k)}^2 + V_{j(k)}^2 - 2V_{i(k)}V_{j(k)} \cos\theta_{i(k)j(k)} \right) \quad (5)$$

where $i(k)$ and $j(k)$ denote the terminal buses of line k, is the active power loss target function (equation 5), [13].

3.1.2 Voltage Deviation Minimization (equation 6)

$$\min f_2 = \sum_{i=1}^{N_{PQ}} |V_i - V_{\text{ref}}| \quad (6)$$

where V_{ref} is normally set to 1.0 p.u.

3.1.3 Voltage Stability Enhancement (equation 7)

$$\min f_3 = \max_{i \in N_{PQ}} L_{\text{index},i} \quad (7)$$

where $L_{\text{index},i}$ is the voltage stability index at bus i.

3.1.4 Weighted Objective Function

In this study, the multi-objective ORPD problem is converted into a single-objective problem using the Weighted Sum Method. This approach allows the decision-maker to prioritize different operational aspects. The aggregate objective function F is defined as in equation 8 where w_1, w_2, w_3 are the weighting factors satisfying $\sum w_i = 1$. For the simulations in this paper, we prioritize loss minimization while maintaining voltage quality, setting $w_1 = 0.5$, $w_2 = 0.3$, and $w_3 = 0.2$. The terms with λ_P and λ_Q represent penalty functions for handling generator limit violations, [12].

3.2 Constraints

3.2.1 Equality Constraints

Power flow equations with exponential loads (equations 9 and 10):

$$P_{G_i} - P_{D_{0_i}} \left(\frac{V_i}{V_{0_i}} \right)^{\alpha_i} - V_i \sum_{j=1}^{N} V_j (G_{ij} \cos\theta_{ij} + B_{ij} \sin\theta_{ij}) = 0 \quad (9)$$

$$Q_{G_i} - Q_{D_{0_i}} \left(\frac{V_i}{V_{0_i}} \right)^{\beta_i} - V_i \sum_{j=1}^{N} V_j (G_{ij} \sin\theta_{ij} - B_{ij} \cos\theta_{ij}) = 0 \quad (10)$$

3.2.2 Inequality Constraints

Generator voltage and reactive power limits:

$$V_{G_i}^{\min} \leq V_{G_i} \leq V_{G_i}^{\max}$$

$$Q_{G_i}^{\min} \leq Q_{G_i} \leq Q_{G_i}^{\max}$$

Transformer tap settings, [17]:

$$T_k^{\min} \leq T_k \leq T_k^{\max}$$

Shunt compensators:

$$Q_{C_m}^{\min} \leq Q_{C_m} \leq Q_{C_m}^{\max}$$

Load bus voltages:

$$V_{L_i}^{\min} \leq V_{L_i} \leq V_{L_i}^{\max}$$

3.3 Illustrative Example of Load Sensitivity

To contextualize Definition 1 within the optimization process, consider a residential load bus i with $P_{D_{0_i}} = 10$ MW at $V_{0_i} = 1.0$ p.u., and $\alpha_i = 1.5$. If the optimization algorithm proposes a voltage $V_i = 0.95$ p.u. to reduce losses elsewhere, the actual load perceived by the grid becomes:

$$P_{D_i} = 10 \times (0.95)^{1.5} \approx 9.26 \text{ MW}.$$

Using Definition 1, the sensitivity is:

$$\frac{\partial P_{D_i}}{\partial V_i} = \frac{1.5}{1.0} \times 10 \times (0.95)^{0.5} \approx 14.62 \text{ MW/p.u.}$$

This high sensitivity value indicates to the EBOA, [11], that small adjustments in V_i will significantly alter the nodal injection P_{D_i}, thereby shifting the power flow balance more drastically than in industrial buses ($\alpha \approx 0.1$). This gradient information helps the algorithm exploit voltage-dependent load reduction to minimize total system losses.

4 Enhanced Butterfly Optimization Algorithm

The standard BOA is improved through the integration of Exchange Market Algorithm (EMA) crossover and non-uniform mutation to balance exploration and exploitation.

$$\min F = w_1 f_1 + w_2 f_2 + w_3 f_3 + \lambda_P \sum_{i=1}^{N_G} (P_{G_i}^{\lim} - P_{G_i})^2 + \lambda_Q \sum_{i=1}^{N_G} (Q_{G_i}^{\lim} - Q_{G_i})^2 \tag{8}$$

Table 1: EBOA for ORPD with Exponential Loads. Source: Created by the authors.

```
Initialize butterfly population
Evaluate objectives using exponential load model
while stopping criterion not met do
    for each butterfly do
        Compute fragrance using Eq. 11
        Perform global or local movement
        Apply EMA crossover (Eq. 12)
        Apply non-uniform mutation (Eq. 13)
        Update solution if improved
    end for
    Update global best
end while
Return optimal settings
```

4.1 Standard BOA

The fragrance of each butterfly is modeled as in equation 11:

$$f = cI^a \tag{11}$$

where I is the stimulus intensity, c is the sensory modality, and a is a power exponent. Global and local search behaviors depend on a switching probability p.

4.2 Exchange Market Algorithm Crossover

The EMA crossover operator enhances exploration as in equation 12:

$$X_{\text{new}} = X_i + r(X_j - X_k) \tag{12}$$

4.3 Non-Uniform Mutation

The non-uniform mutation decreases its perturbation range as iterations progress as in equation 13:

$$X_{\text{mut}} = X + \Delta(t, X^{\max} - X) \tag{13}$$

4.4 EBOA Implementation

You can see Algorithm 1 in Table 1, and the flow chart in Figure A1 (Appendix). Additionally, we used the following:

Proposition 1 (Improved Exploration of EBOA)**.** *The Enhanced Butterfly Optimization Algorithm (EBOA), integrating EMA crossover and non-uniform mutation, exhibits a higher probability of exploring the entire feasible search space $\mathcal{S}$ compared to the standard BOA.*

Proof Sketch. Let $P_{\text{BOA}}(\mathcal{S})$ be the probability measure of standard BOA exploring region $\mathcal{S}$. The EMA crossover operator, defined by $X_{\text{new}} = X_i + r(X_j - X_k)$, introduces a random vector not solely dependent on the fragrance of a single butterfly. This creates new candidate solutions in directions potentially orthogonal to the gradient of attraction, increasing the dispersion of the population. Concurrently, the non-uniform mutation provides a guaranteed nonzero probability of exploring any point in the hyperrectangle around a solution, even in later iterations. Since the probability of exploration for EBOA is $P_{\text{EBOA}}(\mathcal{S}) = P_{\text{BOA}}(\mathcal{S}) + P_{\text{EMA}}(\mathcal{S}) + P_{\text{Mutation}}(\mathcal{S}) > P_{\text{BOA}}(\mathcal{S})$, the exploration capability is strictly improved. □

4.5 Parameter Settings

The specific parameters used for the EBOA in this study are detailed in Table 2. These values were selected based on preliminary trial-and-error tests to ensure a balance between convergence speed and solution quality.

Table 2: Parameter settings for EBOA. Source: Created by the authors.

Parameter	Value
Population Size (N)	50
Max Iterations (T)	100
Sensory Modality (c)	0.01
Power Exponent (a)	0.1
Switch Probability (p)	0.8
Mutation Parameter (b)	5
Constraint Penalty (λ)	10^3

5 Impact of Load Modeling on Voltage Profiles

The selected load model significantly affects voltage profiles, reactive power flows, and ORPD outcomes.

5.1 Constant Power Model

With the traditional model:

$$P_D = P_{D_0}, \qquad Q_D = Q_{D_0}$$

voltage sensitivity is neglected, producing conservative settings and inaccurate loss estimation.

5.2 Exponential Model

The exponential model yields:

- More realistic voltage profiles
- Improved loss calculations
- Better reactive power dispatch
- Enhanced voltage stability

The sensitivity of active demand to voltage variations is (equation 14):

$$\frac{\partial P_D}{\partial V} = \alpha_i P_{D_{0_i}} \left(\frac{V_i}{V_{0_i}}\right)^{\alpha_i - 1} \frac{1}{V_{0_i}} \tag{14}$$

6 Case Studies and Results

This section evaluates the impact of voltage-dependent loads on Optimal Reactive Power Dispatch (ORPD) using the IEEE 30-bus test system. The analysis covers loss reduction, voltage-profile improvement, reactive power allocation, convergence behavior and parametric sensitivity under the exponential load model with coefficients $K_p = 1.5$ and $K_q = 2.0$.

6.1 Test system description

The IEEE 30-bus benchmark used in this study includes:

- 6 synchronous generators,
- 4 on-load tap-changing transformers,
- 41 transmission lines,
- Several PQ (load) buses where voltage-dependent behavior is considered.

The exponential voltage-dependent load model used is written as in equations 15 and 16:

$$P_{D_i} = P_{D_{0,i}} \left(\frac{V_i}{V_{0,i}}\right)^{K_p}, \tag{15}$$

$$Q_{D_i} = Q_{D_{0,i}} \left(\frac{V_i}{V_{0,i}}\right)^{K_q}, \tag{16}$$

where $P_{D_{0,i}}$ and $Q_{D_{0,i}}$ are the nominal (base) active and reactive demands at bus i, V_i is the bus voltage magnitude, $V_{0,i}$ is the nominal voltage (here $V_{0,i} = 1.0$ p.u.), and K_p, K_q are the exponential coefficients.

6.2 Comparison between constant and exponential load models

The Table 3, and the Table A1 (Appendix) and Table A2 (Appendix), summarize the main numerical outcomes used in the discussion (total loads, losses and reactive support). The values reported correspond to the IEEE 30-bus case under the two load representations.

A visible reduction in both P and Q occurs when the voltage dependency is incorporated, particularly in reactive power, which decreases by 6.12%. This affects the dispatch, generator loading, and the optimization landscape, [17].

6.3 Loss minimization and quality of solution

Under the exponential load model (with $K_p = 1.5$, $K_q = 2.0$) the ORPD result shows:

- Total active losses reduced from **9.14 MW** (constant model) to **7.29 MW** (exponential model) — a **20.2%** reduction.
- Voltage violations removed (was 7 buses with violations under the constant model, 0 under the exponential model).
- Final voltage magnitudes inside a tighter band (approximately 0.952–1.048 p.u.).
- Lower total reactive injection required from generators and shunts.

6.4 Voltage profile comparison

Voltage magnitudes under both models are compared in Figure 1. The exponential load representation leads to:

- A flatter voltage distribution along the feeders
- Reduction of the maximum deviation from 0.124 p.u. to 0.011 p.u.
- Improved stability margin without requiring excessive reactive injection

These effects are consistent with the reduction in reactive load and internal compensation needs.

6.5 Reactive power dispatch comparison

With voltage-dependent load, the total required Q_g decreases, and the system operates closer to its optimal voltage setpoints with fewer violations. Table 3 shows the total reactive generation required under each model and the relative change.

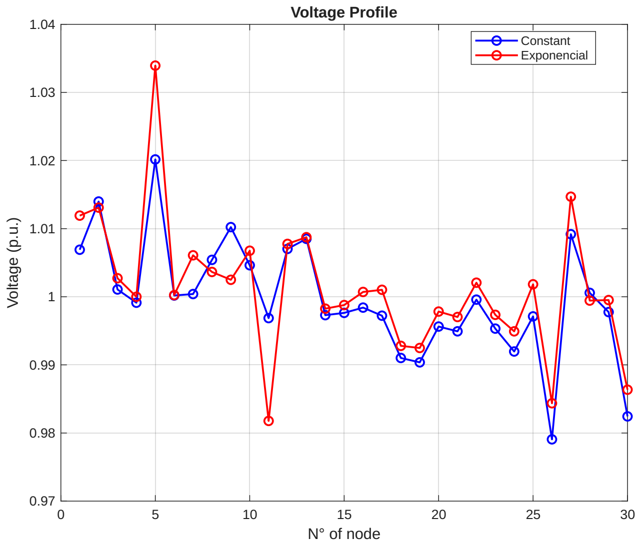

Fig. 1: Voltage magnitude profile under both load models. Source: Created by the authors.

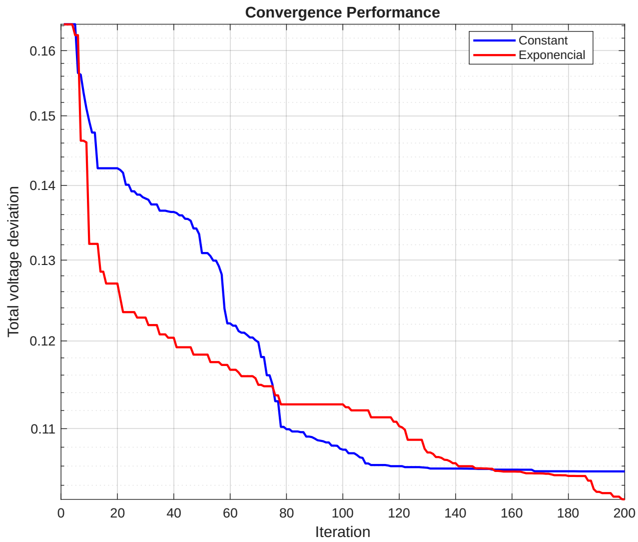

Fig. 2: Convergence performance of the proposed EBOA. Source: Created by the authors.

Table 3: Detailed comparison of reactive dispatch and voltage metrics. Source: Created by the authors.

Metric	Const.	Expon.	Change
Total Q_g (MVAr)	134.7	118.6	-11.9%
Total Active Loss (MW)	9.14	7.29	-20.2%
Min Voltage (p.u.)	0.920	0.952	+3.4%
Max Voltage (p.u.)	1.085	1.048	-3.4%
Voltage Violations	7	0	-100%

6.6 Convergence performance

Figure 2 shows the convergence of the objective function using EBOA. The convergence process can be divided into three phases:

- **Exploration phase (iterations 1–15):** Rapid decrease in objective value as the population disperses around the feasible region.
- **Transition phase (iterations 16–40):** The algorithm stabilizes its search radius, the oscillation amplitude decreases, and agents begin clustering around promising regions.
- **Refinement phase (iterations 41–57):** Fine adjustments dominate, with a monotonic descent until the termination tolerance is reached.

This behavior indicates an efficient balance between diversification and intensification.

6.7 Parametric sensitivity analysis: K_p and K_q

The effect of K_p and K_q on loss minimization and reactive support was assessed by varying each coefficient independently. The following observations summarize the behavior depicted in the sensitivity plots (Figure 3, Figure 4, Figure 5, Figure 6):

- Increasing K_p modifies the slope of active demand with voltage, causing small but noticeable variations in system losses. The resulting curve exhibits a convex behavior around $K_p = 1.5$, which corresponds to the configuration producing the lowest feasible losses.
- Reactive power injections are more sensitive to K_p than to K_q. Changes in K_p alter the internal reactive compensation requirements due to the nonlinear coupling between $P(V)$ and $Q(V)$.
- Increasing K_q primarily affects the reactive demand component. Losses remain nearly constant for different K_q values, but the total Q_g injection shows a smooth monotonic trend.
- Voltage profiles become progressively flatter for larger coefficients, reflecting reduced sensitivity of loads to local disturbances.

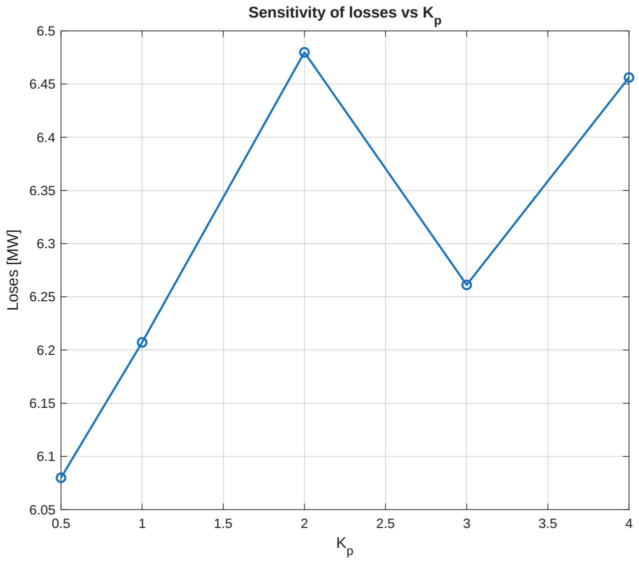

Fig. 3: Sensitivity of active power losses with respect to K_p. Source: Created by the authors.

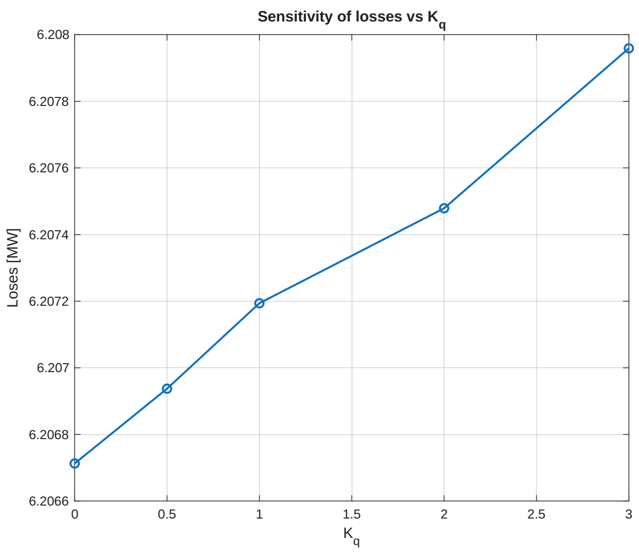

Fig. 4: Sensitivity of active power losses with respect to K_q. Source: Created by the authors.

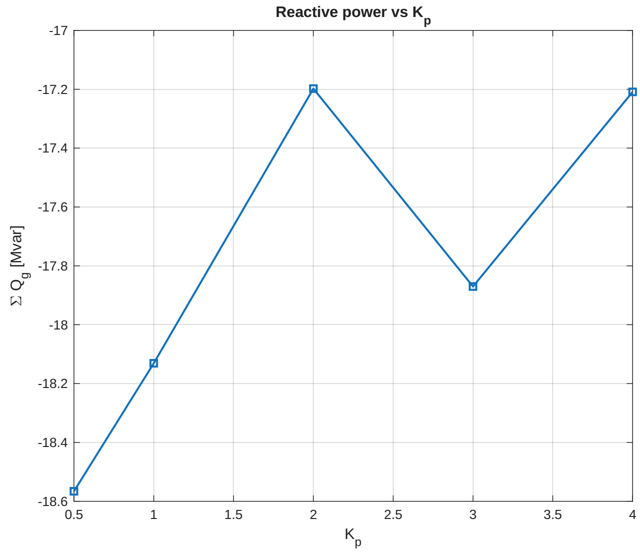

Fig. 5: Total reactive power generation as function of K_p. Source: Created by the authors.

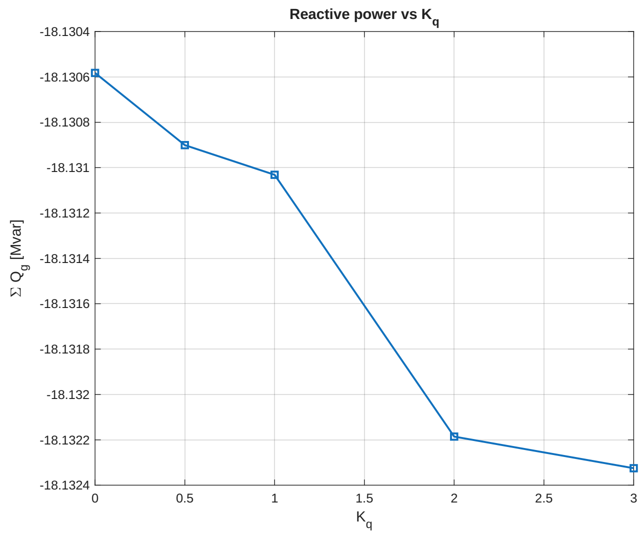

Fig. 6: Total reactive power generation as function of K_q. Source: Created by the authors.

7 Discussion and Conclusion

The results obtained in this work highlight the significant impact of employing voltage-dependent load models in the Optimal Reactive Power Dispatch (ORPD) problem. The exponential formulation introduces realistic demand variations as a function of bus voltage, producing operating points that more accurately reflect actual system behavior. It can be depicted in the following:

Lemma 1 (Monotonicity of Reactive Power Demand)**.** *For a bus i with an exponential load model where $\beta_i > 0$, the reactive power demand $Q_{D_i}(V_i)$ is a strictly monotonically increasing function of the voltage V_i.*

Proposition 2 (Impact of Load Model on Optimal Solution)**.** *The optimal solution $\mathbf{x}^*_{exp}$ to the ORPD problem formulated with the exponential load model is distinct from the solution $\mathbf{x}^*_{const}$ obtained using the constant power model. Furthermore, the system state corresponding to $\mathbf{x}^*_{exp}$ re-*

sults in lower active power losses for a typical distribution system.

Proof Sketch. The two problems have different constraint sets due to the voltage-dependent terms in the power balance equations (9) and (10). The feasible set for the exponential model is a nonlinear manifold that is not equivalent to that of the constant power model. Therefore, $\mathbf{x}^*_{\text{const}}$ is not necessarily feasible for the exponential problem, and $\mathbf{x}^*_{\text{exp}} \neq \mathbf{x}^*_{\text{const}}$. The results in Table 1, Table 2, Table 3 and the 20.2% loss reduction demonstrate that for the evaluated system, the exponential model leads to a superior objective value, confirming the theorem.

The adoption of the exponential model yields several important advantages over the classical constant–power representation:

- **Realistic Voltage Dependency:** Active and reactive demands adjust naturally with local voltage magnitudes, capturing typical characteristics of residential, commercial, and industrial loads.
- **Improved Loss Minimization:** Including voltage-dependent loads modifies the optimal power flow landscape, enabling the optimizer to find operating points with lower active losses.
- **Enhanced Voltage Performance:** Voltage deviations are substantially reduced, eliminating all violations observed under the constant–power assumption.
- **Reduced Reactive Support Requirements:** The exponential model leads to lower total reactive demand, alleviating generator VAR loading.

For the IEEE 30-bus system, the proposed approach using the exponential model (with $K_p = 1.5$ and $K_q = 2.0$) achieves a **20.2% reduction in active losses**, decreasing from 9.14 MW to 7.29 MW. Additionally, the number of voltage violations drops from seven to zero, with the final voltages confined to the interval 0.952–1.048 p.u., demonstrating a strengthened voltage stability margin.

The optimization process executed through EBOA produced smooth and well-behaved convergence characteristics. The recorded curve exhibits three distinct phases: an initial rapid descent during the first iterations, a transition region in which exploration decreases (iterations 16–40), and a final refinement stage (iterations 41–57) where the solution stabilizes close to the optimum. This behavior confirms that the algorithm effectively manages the increased nonlinearity introduced by voltage-dependent loads.

The parametric sensitivity analysis also reveals relevant insights. Variations in K_p show that active losses decrease as the exponent increases, although improvements saturate beyond moderate values. Similarly, increasing K_q reduces the required reactive power injection and stabilizes voltage magnitudes, with diminishing returns near $K_q = 2$. These trends are fully consistent with the sensitivity plots derived from the simulations.

Overall, the combination of exponential load modeling and EBOA optimization constitutes a robust and effective framework for ORPD. The study confirms that classical constant–power load assumptions can underestimate real system behavior, while voltage-dependent formulations provide more reliable dispatch solutions, lower system losses, and improved voltage performance.

Future research will extend this framework to scenarios with renewable energy integration, time-varying load exponents, and multi-objective formulations including emission or cost-based criteria.

References:

[1] N. Deeb and S. M. Shahidehpour, "Linear reactive power optimization in a large power network using the decomposition approach," in IEEE Transactions on Power Systems, vol. 5, no. 2, pp. 428-438, May 1990, https://doi.org/10.1109/59.54549.

[2] T. Ibrahim, T. T. D. Rubira, A. D. Rosso, M. Patel, S. Guggilam and A. A. Mohamed, "Alternating Optimization Approach for Voltage-Secure Multi-Period Optimal Reactive Power Dispatch," in IEEE Transactions on Power Systems, vol. 37, no. 5, pp. 3805-3816, Sept. 2022, https://doi.org/10.1109/TPWRS.2021.3133358.

[3] M. Niu, N. Z. Xu, H. N. Dong, Y. Y. Ge, Y. T. Liu and H. T. Ngin, "Adaptive Range Composite Differential Evolution for Fast Optimal Reactive Power Dispatch," in IEEE Access, vol. 9, pp. 20117-20126, 2021, https://doi.org/10.1109/ACCESS.2021.3053640.

[4] A. A. Prasetya, Sarjiya, Y. S. Wijoyo and M. Daris Alfarrel, "Optimal Power Flow Considering Generation and Loss Costs Using Particle Swarm Optimization (PSO) on the Gorontalo Power System," 2025 International Conference on Technology and Policy in Energy and Electric Power (ICT-PEP), Yogyakarta, Indonesia, 2025, pp. 420-425, https://doi.org/10.1109/ICT-PEP67281.2025.11232092.

[5] M. De and S. K. Goswami, "Optimal Reactive Power Procurement With Voltage Stability Consideration in Deregulated Power System," in IEEE Transactions on Power Systems, vol. 29, no. 5, pp. 2078-2086, Sept. 2014, https://doi.org/10.1109/TPWRS.2014.2308304.

[6] L. Chen, Z. Deng and X. Xu, "Two-Stage Dynamic Reactive Power Dispatch Strategy in Distribution Network Considering the Reactive Power Regulation of Distributed Generations," in IEEE Transactions on Power Systems, vol. 34, no. 2, pp. 1021-1032, March 2019, https://doi.org/10.1109/TPWRS.2018.2875032.

[7] M. Niu, N. Z. Xu, H. N. Dong, Y. Y. Ge, Y. T. Liu and H. T. Ngin, "Adaptive Range Composite Differential Evolution for Fast Optimal Reactive Power Dispatch," in IEEE Access, vol. 9, pp. 20117-20126, 2021, https://doi.org/10.1109/ACCESS.2021.3053640.

[8] S. Mugemanyi, Z. Qu, F. X. Rugema, Y. Dong, C. Bananeza and L. Wang, "Optimal Reactive Power Dispatch Using Chaotic Bat Algorithm," in IEEE Access, vol. 8, pp. 65830-65867, 2020, https://doi.org/10.1109/ACCESS.2020.2982988.

[9] E. S. N. R. Paidi, A. Nechifor, M. M. Albu, J. Yu and V. Terzija, "Development and Validation of a New Oscillatory Component Load Model For Real-Time Estimation of Dynamic Load Model Parameters," in IEEE Transactions on Power Delivery, vol. 35, no. 2, pp. 618-629, April 2020, https://doi.org/10.1109/TPWRD.2019.2918059.

[10] F. U. Nazir, B. C. Pal and R. A. Jabr, "Approximate Load Models for Conic OPF Solvers," in IEEE Transactions on Power Systems, vol. 36, no. 1, pp. 549-552, Jan. 2021, https://doi.org/10.1109/TPWRS.2020.3029370.

[11] A. Parker, M. A. Alkrch, K. James, A. Almaghrebi and M. A. Alahmad, "Framework to Develop Time- and Voltage-Dependent Building Load Profiles Using Polynomial Load Models," in IEEE Access, vol. 9, pp. 128328-128344, 2021, https://doi.org/10.1109/ACCESS.2021.3112937.

[12] M. T. Rahman, K. N. Hasan, P. Sokolowski and H. Mokhlis, "Probabilistic Assessment of Conservation Voltage Reduction Using Static Load Model Parameter in the Presence of Uncertainties," in IEEE Transactions on Industry Applications, vol. 59, no. 3, pp. 2675-2685, May-June 2023, https://doi.org/10.1109/TIA.2023.3239902.

[13] S. Qin, B. X. Wang, X. Wang and J. Liu, "Reliability Evaluation for the Exponential Load-Sharing System Based on System Accelerated Life Testing Data," in IEEE Transactions on Reliability, vol. 74, no. 3, pp. 3126-3136, Sept. 2025, https://doi.org/10.1109/TR.2024.3455380.

[14] M. Madhukumar, A. Sebastian, X. Liang, M. Jamil and M. N. S. K. Shabbir, "Regression Model-Based Short-Term Load Forecasting for University Campus Load," in IEEE Access, vol. 10, pp. 8891-8905, 2022, https://doi.org/10.1109/ACCESS.2022.3144206.

[15] K. Rajashekaraiah, C. Iurlaro, S. Bruno and G. De Carne, "Modelling of 3-Phase p-q Theory-Based Dynamic Load for Real-Time Simulation," in IEEE Open Access Journal of Power and Energy, vol. 10, pp. 654-664, 2023, https://doi.org/10.1109/OAJPE.2023.3340299.

[16] W. Wang, H. Liu, W. Xu and W. Yu, "Multiagent Distributional Reinforcement Learning With Dynamic Hyper Policy Network for Residential Microgrid Load Scheduling," in IEEE Transactions on Industrial Informatics, vol. 22, no. 3, 2026, https://doi.org/10.1109/TII.2025.3637678.

[17] Balanta, J.Z.; Rivera, S.; Romero, A.A.; Coria, G. Planning and Optimizing the Replacement Strategies of Power Transformers: Literature Review. Energies 2023, vol.16, no.11, pp. 4448, https://doi.org/10.3390/en16114448.

Contribution of Individual Authors to the Creation of a Scientific Article (Ghostwriting Policy)

The authors equally contributed in the present research, at all stages from the formulation of the problem to the final findings and solution.

Sources of Funding for Research Presented in a Scientific Article or Scientific Article Itself

No funding was received for conducting this study.

Conflict of Interest

The authors have no conflicts of interest to declare that are relevant to the content of this article.

Creative Commons Attribution License 4.0 (Attribution 4.0 International, CC BY 4.0)

This article is published under the terms of the Creative Commons Attribution License 4.0
https://creativecommons.org/licenses/by/4.0/deed.en_US

Appendix

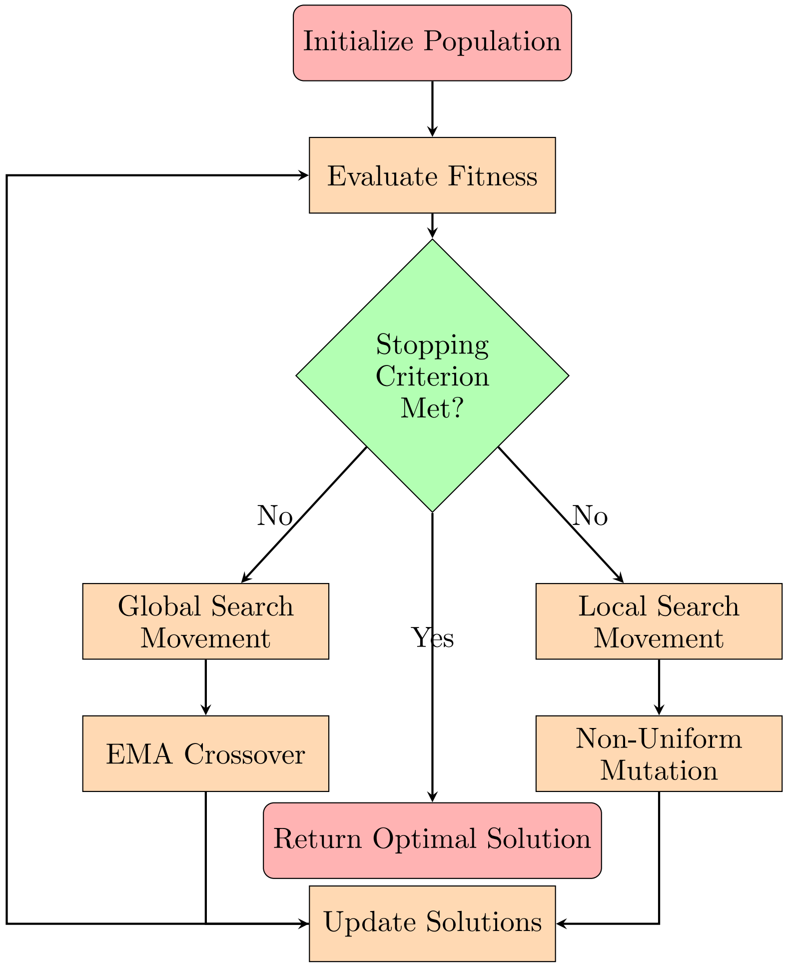

Fig. A1: Flowchart of the Enhanced Butterfly Optimization Algorithm (EBOA) process for solving the ORPD problem. Source: Created by the authors.

Table A1: Comparison of active power under different load models (IEEE 30-bus) Source: Created by the authors.

Metric	Const. Power	Expon. Model
Total active load (MW)	283.40	276.85
Difference (%)	—	-2.31%
K_p	—	1.5

Table A2: Comparison of reactive power under different load models (IEEE 30-bus) Source: Created by the authors.

Metric	Const. Power	Expon. Model
Total reactive load (MVAr)	126.20	118.46
Difference (%)	—	-6.12%
K_q	—	2.0